COMPRESSED SENSING FOR DIGITAL HOLOGRAPHIC MICROSCOPY

Marcio M. Marim[1,3]*, Michael Atlan*[2]*, Elsa D. Angelini*[3]*, J.-C. Olivo-Marin*[1]

[1]Institut Pasteur, Unité d'Analyse d'Images Quantitative CNRS URA 2582, F-75015 Paris
[2]Institut Langevin. ESPCI ParisTech - CNRS UMR 7587, INSERM U 979, UPMC, UP7. F-75005 Paris
[3]Institut Télécom, Télécom ParisTech CNRS LTCI, F-75013 Paris

ABSTRACT

This paper describes an original microscopy imaging framework successfully employing Compressed Sensing for digital holography. Our approach combines a sparsity minimization algorithm to reconstruct the image and digital holography to perform quadrature-resolved random measurements of an optical field in a diffraction plane. Compressed Sensing is a recent theory establishing that near-exact recovery of an unknown sparse signal is possible from a small number of non-structured measurements. We demonstrate with practical experiments on holographic microscopy images of cerebral blood flow that our CS approach enables optimal reconstruction from a very limited number of measurements while being robust to high noise levels.

Index Terms— Compressed Sensing, digital holography, biological microscopy, signal reconstruction

1. INTRODUCTION

Digital holographic microscopy (DHM) provides quantitative phase contrast imaging, high resolution, non-destructivity and multi-focus representation of the specimen [1]. In biology, this technique is suitable for marker-free analysis of living cells. However, general high resolution microscopy involves dense data acquisition. Reducing the number of pixels to read out or simply increasing the throughput is commonly targeted for improving image acquisition and analysis rate. One intense field of research aims to reduce the amount of data acquisition or sample illumination [2, 3]. In [2], the acquisition is restricted to only those areas where relevant signal is present. In [3] a method called controlled light-exposure microscopy (CLEM) is introduced, supported by a nonuniform illumination of the field of view. However, both methods suffer from being image-content dependent for a successful implementation. Indeed, these methods need a feedback loop inside the acquisition setup to make decisions about the sampling rate or the illumination intensity, depending on the objects characteristics.

This article attempts to address the sensing problem in DHM by increasing the detection throughput via the concept and preliminary results of an actual *Compressed Sensing* (CS) implementation. This method is independent of image-content and does not need any feedback loop during the acquisition. CS was previously reported in MRI acquisition [4] or digital imaging [5]. The main idea behind this work is to perform very few measurements with digital holography and solve a direct optimization problem to reconstruct the image. In microscopy, the observation of detailed target structures is also challenged by poor signal quality since smaller exposure times, required for fast acquisition rates, provide low signal-to-noise ratio (SNR) images.

This work was funded by Institut Pasteur, DGA, Institut Langevin, ANR and CNRS. The authors also acknowledge support from Fondation Pierre-Gilles de Gennes. Corresponding authors:
Marcio Marim: marim@pasteur.fr
J-C Olivo-Marin: jcolivo@pasteur.fr, www.bioimageanalysis.org

2. METHODS

CS is a novel mathematical theory for sampling and reconstructing signals in a efficient way, introduced by Candès and Donoho [6, 7]. It exploits the fact that most images are compressible or sparse in some domain due to the homogeneity, compactness and regularity of structures. Instead of sampling the entire data and then compress it to eliminate redundancy, CS performs a compressed data acquisition. Some basic requirements to enable Compressed Sensing are (i) to find a sparsifying transform able to shrink the data into a small number of coefficients (ii) to acquire random projections of the signal into orthogonal subspaces, such as the Fourier domain for spatially-sparse images (iii) to use a sampling scheme that obeys the Restricted Isometry Property (RIP) [8] and (iv) to use a sampling domain and a sparsifying transform that span incoherent domains [9].

Complying with these requirements, CS states that a signal $g \in \mathbb{R}^N$ having a S-sparse representation (i.e. it can be well represented by a small number S of coefficients, where $S \ll N$) on a basis Ψ, can be reconstructed very accurately from a small number of projections of g onto randomly chosen subsets of vectors in the measurement subspace (e.g. Fourier measurements for spatial sparsity). More precisely, a signal g has a sparse representation if it can be written as a linear combination of a small set of vectors taken from some basis Ψ, such as $g = \sum_i^N c_i \Psi_i$, with $\| c \|_{\ell_1} \approx S$, where $\| \cdot \|_{\ell_1}$ denotes the ℓ_1 norm which corresponds to the sum of magnitudes of all terms of the candidate signal g projected on Ψ. More precisely, a more exact measure of sparsity of g is given by the ℓ_0 norm of g, which is not exactly a norm but the number of non-zero coefficients of g. However, we use the ℓ_1 norm which in practice gives a very accurate estimation of sparsity. In general, the ℓ_p norm is defined as:

$$\| \mathbf{c} \|_{\ell_p} := \{ \sum_{i=1}^{N} |c_i|^p \}^{1/p} \tag{1}$$

As demonstrated in [10], if such a sparsifying transform Ψg exists in the spatial domain, it is possible to reconstruct an image g from partial knowledge of its Fourier spectrum. In holographic microscopy, g will represent the local optical intensity in the object

plane. We denote $f \in \mathbb{C}^N$ the associated complex optical field, satisfying $g = |f|^2$. The radiation field propagates from the object to the detector plane in Fresnel diffraction conditions. Thus, the optical field in the object plane f is linked to the field F in the detection plane by a Fresnel transform, expressed in the discrete case as:

$$\begin{aligned} F &= \mathcal{F}(f) : \mathbb{C}^N \to \mathbb{C}^N \\ F_p &= \frac{1}{N} \sum_{n=1}^{N} f_n \, \mathrm{e}^{i\left(\alpha n^2 - 2\pi np/N\right)} \end{aligned} \tag{2}$$

where $n, p \in \{1, \ldots, N\}$ denote pixel indexes, $\alpha \in \mathbb{R}^+$ is the parameter of the quadratic phase factor $\mathrm{e}^{i\alpha n^2}$ describing the curvature in the detection plane of a wave emitted by a point source in the object plane. In CS, the signal reconstruction consists in solving a convex optimization problem that finds the candidate $\hat{g}$ ($\hat{\cdot}$ denotes an estimator) of minimal complexity satisfying $\hat{F}|_\Gamma = F|_\Gamma$, where $F|_\Gamma \subseteq F$ is a partial subset of measurements in the set Γ.

2.1. Digital Holography

The experimental setup is sketched in Fig. 1. It consists of an off-axis, frequency-shifting digital holography scheme [11, 1]. The monochromatic optical field from a near infrared diode laser illuminates the skull of an adult mouse, anesthetized with a mixture of xylazine and ketamine (1 mg/kg IP, 10 mg/kg IP), positioned on a stereotaxic frame. Cranial skin and subcutaneous tissue were excised linearly over the sagittal suture and cortical bones were preserved. The backscattered field beats against a separate local oscillator (LO) field detuned by $\Delta\omega/(2\pi) = 30\,\mathrm{Hz}$ and creates a time-fluctuating interference pattern measured with a $N = 1024 \times 1024$ array detector. The diffracted object field map in the detector plane, resolved in quadrature (in amplitude and phase) $F \in \mathbb{C}^N$ is calculated from a four-phase measurement [11]. The frequency detuning $\Delta\omega$ enables rejection of non fluctuating light components reflected by the preparation as well as speckle reduction through signal accumulation.

F can be back-propagated numerically to the target plane with the standard convolution method when all measurements $F \in \mathbb{C}^N$ are available. In this case, the complex field in the object plane f is retrieved from a discrete inverse Fresnel transform of F; $f = \mathcal{F}^{-1}(F)$:

$$f_p = \frac{1}{N} \sum_{n=1}^{N} F_n \, \mathrm{e}^{-i\left(\alpha n^2 - 2\pi np/N\right)} \tag{3}$$

2.2. CS reconstruction

Now returning to the CS reconstruction problem, we want to recover the intensity image of the object $g = \{|f|^2 : f \in \mathbb{C}^N\}$ from a small number of measurements $F|_\Gamma \in \mathbb{C}^M$ where $M \ll N$. Partial measurements in the detection plane can be written as $F|_\Gamma = \Phi f$, where the sampling matrix Φ models a discrete Fresnel transform described in (2) and random undersampling with flat distribution. To find the best estimator $\hat{g}$, we solve the following convex optimization problem [10]:

$$\hat{g} = \arg\min_{g \in \mathbb{R}^N} \| \Psi g \|_{\ell_1} \text{ subject to } \hat{F}|_\Gamma = F|_\Gamma \tag{4}$$

Explicitly, given a partial knowledge of the Fresnel coefficients $F|_\Gamma$, we seek a solution $\hat{g}$ with maximum sparsity (i.e. with minimal norm $\| \Psi g \|_{\ell_1}$), and whose Fresnel coefficients $\hat{F}|_\Gamma$ match the subset observed $F|_\Gamma$. Since our test image is piecewise constant with sharp edges (such as most microscopy images), it can be sparsely represented computing its gradient. In this case, sparsity is expressed with the Total Variation (TV) measure of the image:

$$\begin{aligned} \| g \|_{TV} &= \| \nabla g \|_{\ell_1} \\ &= \sum_{i,j} \sqrt{\{g_{i+1,j} - g_{i,j}\}^2 + \{g_{i,j+1} - g_{i,j}\}^2} \end{aligned} \tag{5}$$

The incoherence property holds for the two basis adopted here, which are the Fresnel spectrum and the TV [9]. Moreover, random measurements in the spectral domain satisfy the RIP condition [10]. Hence for overwhelming percentage of Fresnel coefficients sets Γ with cardinality obeying $|\Gamma| = M \geq K \cdot S \log N$, for some constant K, $\hat{g}$ is the unique solution to the problem :

$$\hat{g} = \arg\min_{g \in \mathbb{R}^N} \| \nabla g \|_{\ell_1} \text{ s.t. } \hat{F}|_\Gamma = F|_\Gamma \tag{6}$$

However, holographic measurements are corrupted with noise and the observed signal is not exactly sparse. More appropriately, the observations can be described by noisy measurements $F|_\Gamma = \Phi f + n$, where $n \in \mathbb{C}^M$ is a noise component with bounded energy $\| n \|_{\ell_2} \leq \epsilon$. In this particular case, a better reconstruction can be achieved by relaxing the constraint $\hat{F}|_\Gamma = F|_\Gamma$ and allowing an error δ at most proportional to the noise energy ϵ [12, 13]. Finally, solving the following problem performs the reconstruction of g with robustness to noise:

$$\hat{g} = \arg\min_{g \in \mathbb{R}^N} \| \nabla g \|_{\ell_1} \text{ s.t. } \| \hat{F}|_\Gamma - F|_\Gamma \|_{\ell_2} \leq \delta \tag{7}$$

for some $\delta \leq C\epsilon$, which depends on the noise energy. The problem (7) is recast as a second-order cone problem (SOCP) and the SOCP is then solved with a generic log-barrier algorithm [7].

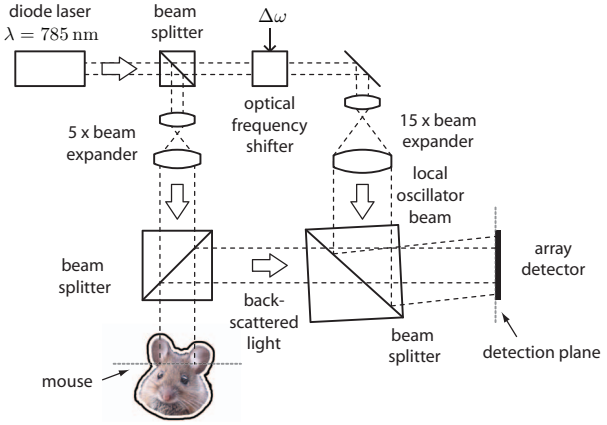

Fig. 1: Sketch of the holographic microscopy experimental image acquisition setup.

3. EXPERIMENTS AND RESULTS

3.1. Analysis of denoising capability

In this subsection we analyze the denoising capability of the method described in (7). The robustness to noise relies on the efficiency of the sparsity transform on representing well the signal of interest and on representing inefficiently the noise distribution. In the context

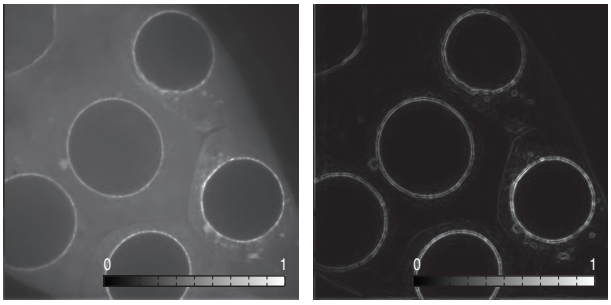

(a) $\| \nabla f \|_{\ell_1} = 28 \times 10^3$ (b) $\| \nabla f \|_{\ell_1} = 3 \times 10^3$

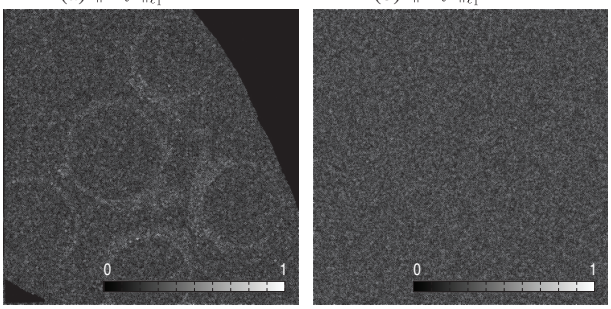

(c) $\| \nabla f \|_{\ell_1} = 22 \times 10^3$ (d) $\| \nabla f \|_{\ell_1} = 19 \times 10^3$

Fig. 2: Sparsifying transformation $\| \nabla f \|_{\ell_1}$, (a) noisy microscopy image, (b) noise-free image (compressible signal of interest), (c) Poisson noise component and (d) Gaussian noise component.

of microscopic images, noise models usually combine Poisson and Gaussian components. We performed here an analysis of the sparsity of each noise component by adding a mixture of Poisson and Gaussian noise to a fluorescence microscopy image of drosophyla cell and applying the sparsifying transform to noise components independently, results to this experience are illustrated in Fig. 2. Fig. 2(a) is the noisy microscopy image, 2(b) shows the magnitude of the gradient of the noise-free image (compressible signal of interest). 2(c) shows the magnitude of the gradient of the Poisson noise component and 2(d) shows the magnitude of the gradient of the Gaussian noise component. The value $\| \nabla f \|_{\ell_1}$ correspond to the measure of sparsity. In both cases, the coefficients provided by the transformation are not sparse or strongly less sparse than in Fig. 2 (for the signal of interest). These results show clearly that the sparsifying transform used does not encode efficiently the noise, which is strongly suited for a denoising framework. Moreover we can observe that the signal of interest is very efficiently encoded by the transformation.

3.2. Holographic microscopy image reconstruction

In Fig. 3 we illustrate some CS reconstruction results. A reconstruction of an off-axis image with the standard convolution method described in (3) is illustrated in Fig. 3(a). The image reconstructed with holography uses all available measurements (4 phases $\times$ 20 accumulations $\times 1024^2 = 8.4 \times 10^7$ pixels). For the CS approach, Fresnel coefficients are undersampled randomly. Fig. 3(b) shows the CS exact recovery such as described in (6) and Fig. 3(c) shows the CS recovery with the constraint relaxation such as described in (7). For both CS reconstruction we use only 7% of the pixels used in the standard approach (4 phases $\times$ 20 accumulations $\times$ 0.07 $\times 1024^2 = 5.8 \times 10^6$ pixels). Figs. 3(d)-(f) display magnified views from central region of images (a-c), illustrating the quality of the reconstruction. Fig. 3(g) illustrates the gradient of the image ∇g, corresponding to the sparse domain. Finally, Figs. 3(h) and 3(i) illustrates the residual (Euclidean distance $|\hat{g} - g|$) from standard holographic reconstruction (a) and CS reconstructions (b) and (c). This error in Fig. 3(i) is essentially due to the relaxation of the constraint for a perfect match between measures and estimations in the CS scheme, leading to some denoising effect, confirmed by the visual aspect of the residual image image Fig. 3(i) showing essentially unstructured noise.

4. CONCLUSION

We have presented a novel microscopy imaging framework successfully employing Compressed Sensing principles. It combines an iterative image reconstruction and digital holography to perform quadrature-resolved random measurements of an optical field in a diffraction plane. The CS approach enables optimal image reconstruction while being robust to high noise levels. The proposed technique is expected to greatly improve many microscopy applications, allowing the acquisition of high dimensional data with reduced acquisition time and opening the door to new acquisition protocols.

5. REFERENCES

[1] M. Gross and M. Atlan, "Digital holography with ultimate sensitivity," *Optics Letters*, vol. 32, pp. 909–911, 2007.

[2] C. Jackson, R. Murphy, and J. Kovačević, "Intelligent acquisition and learning of fluorescence microscope data models," *IEEE Transactions on Image Processing*, vol. 18, pp. 2071–2084, September 2009.

[3] R. Hoebe, C. Van Oven, T. Gadella Jr, P. Dhonukshe, C. Van Noorden, and E. Manders, "Controlled light-exposure microscopy reduces photobleaching and phototoxicity in fluorescence live-cell imaging," *Nature Biotechnology*, vol. 25, pp. 249–253, 2007.

[4] M. Lustig, D. Donoho, and J. M. Pauly, "Sparse MRI: The application of compressed sensing for rapid MR imaging," *Magnetic Resonance in Medicine*, vol. 58(6), pp. 1182–1195, 2007.

[5] D. Takhar, J. Laska, M. Wakin, M. Duarte, D. Baron, S. Sarvotham, K. Kelly, and R. Baraniuk, "A new compressive imaging camera architecture using optical-domain compression," *IS&T/SPIE Computational Imaging IV*, vol. 6065, 2006.

[6] D. L. Donoho, "Compressed Sensing," *IEEE Trans. on Information Theory*, vol. 52(4), pp. 1289–1306, April 2006.

[7] E. Candès and J. Romberg, "Practical signal recovery from random projections," *Proc. SPIE, Wavelet Applications in Signal and Image Processing XI*, 2005.

[8] E. Candès, "The restricted isometry property and its implications for Compressed Sensing," *Compte Rendus de l'Academie des Sciences, Paris*, vol. Serie I, pp. 346 589–592, 2008.

[9] E. Candès and J. Romberg, "Sparsity and incoherence in Compressive Sampling," *Inverse Problems*, vol. 23(3), pp. 969–985, 2006.

[10] E. Candès, J. Romberg, and T. Tao, "Robust uncertainty principles: Exact signal reconstruction from highly incomplete frequency information," *IEEE Trans. on Information Theory*, vol. 52(2), pp. 489–509, 2006.

[11] M. Atlan and M. Gross, "Spatiotemporal heterodyne detection," *Journal of the Optical Society of America A*, vol. 24, no. 9, pp. 2701–2709, 2007.

[12] M. Marim, E. Angelini, and J.-C. Olivo-Marin, "A Compressed Sensing approach for biological microscopic image processing," *IEEE International Symposium on Biomedical Imaging, ISBI*, pp. 1374–1377, 2009.

[13] D. Donoho, M. Elad, and V. Temlyakov, "Stable recovery of sparse overcomplete representations in the presence of noise," *IEEE Trans. on Information Theory*, vol. 52, pp. 6–18, 2006.

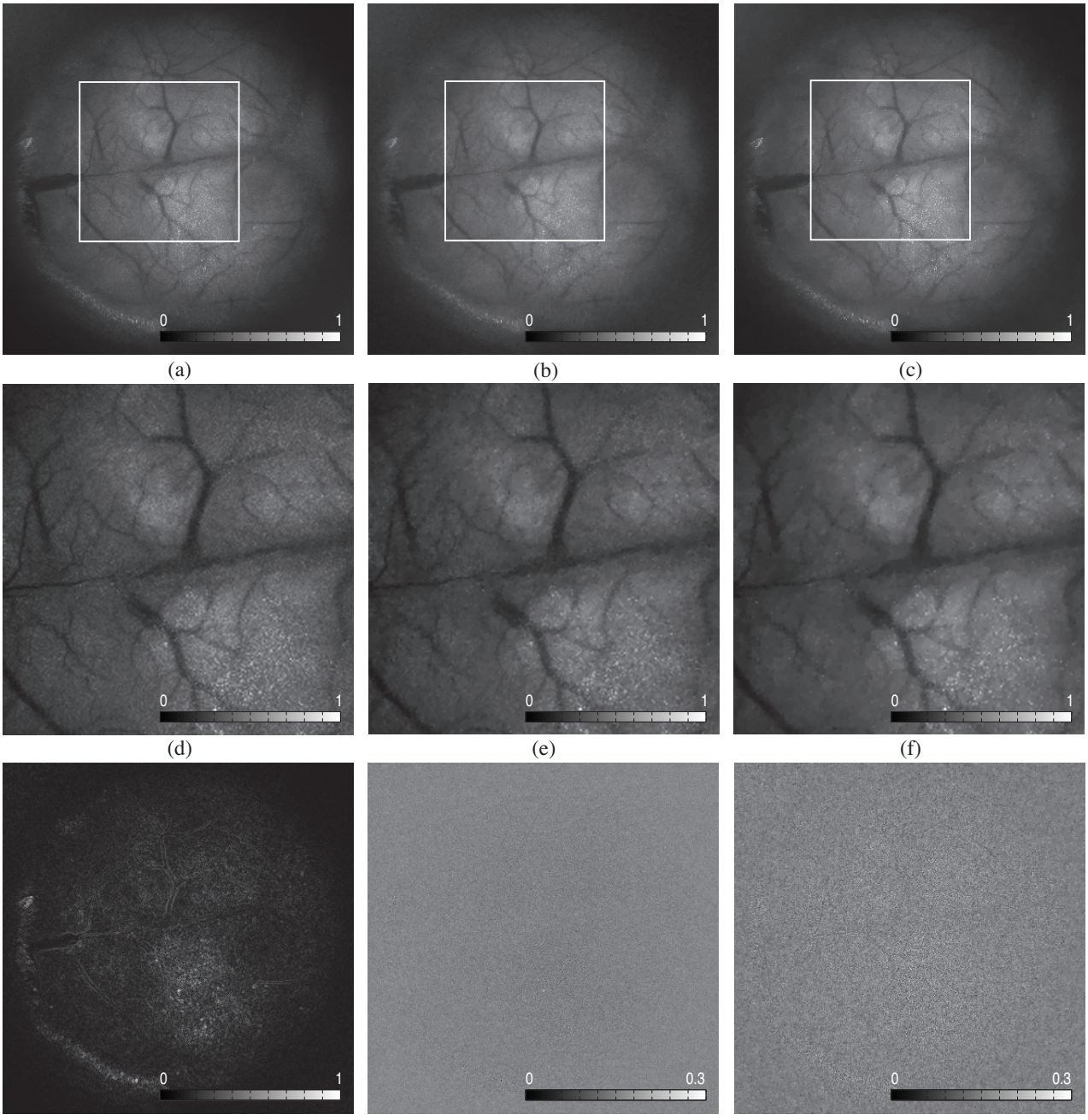

Fig. 3: Mouse cerebral blood flow (CBF) imaged by digital holography (a) Standard holographic reconstruction, as described in (2). (b) CS exact recovery, using 7% of the Fresnel coefficients acquired with holography, as described in (6). (c) CS recovery with denoising, as described in (7). (d-f) Magnified views from (a-c). (g) Gradient of (a). (h) Residual from $|$(a)-(b)$|$. (i) Residual from $|$(a)-(c)$|$.